

Cucurbit[7]uril as Host of Adamantane-Modified Dyes for Fluorescence Enhancement in Aqueous Environment

Hong-Jiao Liu,^a Guo-Wei Chen,^a Ru Sun^{*,a} and Jian-Feng Ge^{*,a,b}

^a College of Chemistry, Chemical Engineering and Material Science, Soochow University, 199 Ren' Ai Road, Suzhou 215123, China.

^b Jiangsu Key Laboratory of Medical Optics, Suzhou Institute of Biomedical Engineering and Technology, Chinese Academy of Sciences, Suzhou 215163, China.

Index

1. Experimental section	S1
1.1. Materials and instruments.....	S1
1.2. Preparation of test solution and photostability experiment	S1
1.3. Determination of fluorescence quantum yields and fluorescence lifetime	S2
1.4. Determination of the inclusion equilibrium constant.....	S2
1.5. Cell culture and imaging	S3
1.6. Computational details.....	S3
2. Tables	S4
Table S1. The electron cloud distribution for the HOMO and LUMO, energy gap and dipole moments of NR-Ad , CB[7] and NR-Ad@CB[7]	S4
Table S2. Optical properties of dye LDs-NPAd2 in water before and after adding CB[7] or CB[8]	S4
3. Figures	S5
Fig. S1. Fluorescence decay spectra of dyes Coum-Ad (a), LDs-NPAd1 (b), NR-Ad (c) before and after the addition of CB[7] in PBS.	S5
Fig. S2. UV-Vis absorption spectra and standard curves of dyes in different concentrations. (a, b) Coum-Ad ; (c, d) LDs-NPAd1 ; (e, f) NR-Ad	S6

* Corresponding authors. E-mail addresses: sunru924@hotmail.com (R. Sun), gejianfeng@hotmail.com (J.-F. Ge).

Fig. S3. Absorption spectra of dyes Coum-Ad (a), LDs-NPAd1 (b), NR-Ad (c) with the concentration of 1 μM in different ratios of CB[7] solution. Inset: photographs in sunlight.	S6
Fig. S4. Fluorescence decay spectrum of dye LDs-NPAd2 before and after the addition of CB[8] in PBS.	S7
Fig. S5. Absorption spectrum of dye LDs-NPAd2 with the concentration of 1 μM in different ratios of CB[8] solution. Inset: photograph in sunlight.....	S7
Fig. S6. Photostability of dyes Coum-Ad , LDs-NPAd1 , NR-Ad and LDs-NPAd2 with the presence and absence of CB[n] in acetonitrile.	S8
Fig. S7. Selective experiments of dyes Coum-Ad (a), LDs-NPAd1 (b), NR-Ad (c), LDs-NPAd2 (d) with concentration of 1 μM toward different analytes (100 μM) in PBS containing 1% DMSO before and after the addition of CB[7] (2 μM) or CB[8] (20 μM). 1: Blank, 2: Ba^{2+} , 3: Cd^{2+} , 4: Co^{2+} , 5: Cu^{2+} , 6: Mn^{2+} , 7: Ni^{2+} , 8: Pd^{2+} , 9: K^+ , 10: CO_3^{2-} , 11: SO_4^{2-} , 12: Cys, 13: Gly, 14: Lys. Coum-Ad was excited at 380 nm, slit widths: 5 nm/3 nm; LDs-NPAd1 was excited at 466 nm, slit widths: 5 nm/3 nm; NR-Ad was excited at 605 nm, slit widths: 5 nm/3 nm; LDs-NPAd2 was excited at 440 nm, slit widths: 5 nm/3 nm. The data were shown as mean \pm SD ($n = 3$).	S9
Fig. S8. Cell viabilities of living HeLa cells incubated with dyes in different concentration gradients (0, 2, 4, 6, 8 and 10 μM) before and after the addition of CB[7] (2 eq) or CB[8] (20 eq). The data were shown as mean \pm SD ($n = 3$).	10
Fig. S9. Colocalization images of living HeLa cells with dyes (0.5 μM), CB[7] (1.0 μM) or CB[8] (10 μM) and corresponding commercial organelle-makers. (a1-a3) The brightfield images of living HeLa cells; (b1-b3) confocal images in red channel; (c1-c3) confocal images in green channel; (d1-d3) The merged images of (b1-b3) and (c1-c3); (e1-e3) The fluorescent intensity for the linear regions of interest (ROIs); (f1-f3) The fluorescent intensity correlation plots.....	S10
4. References	S11

1. Experimental section

1.1. Materials and instruments

Unless otherwise stated, all reagents were purchased from Aladdin, Macklin or Qiangsheng (Suzhou, China) and used without further purification. Notably, the CB[7] and CB[8] used in this work were sourced from Macklin (98%) without residual water. Molecular weights are 1162.96 g/mol and 1329.1 g/mol, respectively. Silica gel (200–300 mesh) was used to purify the product by flash chromatography. The preparation of dyes **Coum-Ad**, **LDs-NPAds** and **NR-Ad** were based on the reported work.¹

Melting points were determined on an X-4 microscope electron thermal apparatus (Kerui, China). Infrared spectra were obtained at a Bruker VERTEX70 IR spectrometer. ¹H NMR spectra (300 MHz) and ¹H NMR (600 MHz) spectra were separately measured with Varian and Bruker nuclear magnetic resonance apparatus at room temperature. Mass spectra were obtained by using Xevo G2-XS TOF or MicroQ-TOF mass spectrometer. UV–vis absorption spectra were obtained with a Shimadzu UV-1800 spectrometer and emission spectra were carried out on Shimadzu RF-5301PC spectrometer in fused quartz cuvettes (10 mm × 10 mm) at room temperature. Fluorescence quantum yields were measured by Shimadzu UV-1800 spectrometer to determine the excitation wavelength and Shimadzu RF-5301PC spectrometer to obtain corrected emission spectra. According to standard equation and fluorescence quantum yields of known compounds (the section 1.3), values of fluorescence quantum yield were obtained. The fluorescence decay spectra were measured by using an Edinburgh FLS1000 fluorescence spectrophotometer. A Leica TCS SP5 II confocal laser scanning microscope was operated to record the fluorescence confocal images, and the images were processed with LAS-AF lite software.

1.2. Preparation of test solution and photostability experiment

The stock solutions of all dyes (1 mM) were prepared in DMSO. The stock solutions of CB[7] (100 μM) and CB[8] (200 μM) were prepared in PBS (pH = 7.4). Different interfering substances (including K₂CO₃, BaCl₂, CdCl₂, CoCl₂, CuSO₄, MnCl₂, NiCl₂, PbCl₂, Cys, Gly, Lys) were dissolved in twice distilled water to prepare the stock

solutions (10 mM). The stock solutions were further diluted to the required concentration for test. All test solutions contained 1% DMSO unless otherwise stated. The test solutions for photostability were prepared from acetonitrile containing dyes (10 μ M) and different host (10 μ M). And they were continuously irradiated with 500 W of Philips iodine-tungsten lamp for 200 min. Meanwhile, the distance between the irradiated sample and the lamp remained 25 cm, and an 8 cm thick cold trap prepared by NaNO₂ (60 g/L) was placed between them in order to eliminate the interference of heat and short wavelength light. The absorbance of the absorption maximum at different times was recorded, and the remaining absorbance (%), a parameter reflecting the trend of photostability, was calculated according to the recorded change of absorbance.

1.3. Determination of fluorescence quantum yields and fluorescence lifetime

All the relative fluorescence quantum yields were calculated by the following equation:

$$\Phi_x/\Phi_t = [A_{st}/A_x][n_x^2/n_{st}^2][D_x/D_{st}]$$

Where st: standard; x: sample; Φ : quantum yield; A: absorbance at the excitation wavelength; D: area under the fluorescence spectra on an energy scale; n: the refractive index of the solution. Harmine hydrochloride ($\Phi = 0.45$ in 0.1 M H₂SO₄), Coumarin-153 ($\Phi = 0.547$ in ethanol) and Cresyl violet ($\Phi = 0.578$, in ethanol) were used as standard for different dyes.^{2, 3}

All the relative fluorescence lifetimes were calculated by the following equation:

$$\tau_{ave} = [A_1\tau_1^2 + A_2\tau_2^2]/[A_1\tau_1 + A_2\tau_2]$$

Where A₁, τ_1 , A₂, τ_2 were derived from the nonlinear fitting of the fluorescence decay spectra.

1.4. Determination of the inclusion equilibrium constant

Different concentration of CB[n] solutions ranging from 0 μ M to 30 μ M were prepared in PBS. The inclusion equilibrium constant between dyes and CB[n] was

measured by the Benesi-Hildebrand equation which is as follows:

$$\frac{1}{(F - F_0)} = \frac{1}{(F' - F_0)} + \frac{1}{(F' - F_0)K[CB[n]]}$$

Where “K” is the inclusion equilibrium constant, F_0 is the fluorescence intensity of dyes (1 μM) without CB[n] in water, F is that with CB[n] in water at a specified concentration, and F' is that when all of molecules are effectively complexed. [CB[n]] is the corresponding concentration of CB[n] in test solution.

1.5. Cell culture and imaging

HeLa cells were cultured in Roswell Park Memorial Institute culture medium (RPMI-1640) which contained L-glutamine (2.5×10^{-4} M), 10% calf serum, streptomycin ($100 \mu\text{g mL}^{-1}$) and penicillin (100 U mL^{-1}). The incubator contained CO_2 : air (5:95) at 37 °C. Before the cell experiments, the HeLa cells were attached to glass-bottomed coverslips and cultivated for two days. The CCK-8 method was used to assess cytotoxicity of dyes and CB[n].

In the response experiments, living HeLa cells were incubated with **NR-Ad** (0.5 μM) and CB[7] (1 μM), **LDs-NPAd1** (0.5 μM) and CB[7] (1 μM) or **LDs-NPAd2** (0.5 μM) and CB[8] (10 μM) for 10 min, respectively. HeLa cells in the control group were cultured with dyes (0.5 μM) for 10 min. After the HeLa cells were rinsed three times with PBS, the images were captured. The red channel images were achieved between 600 nm and 700 nm at 561 nm excitation, and the green channel images were acquired between 500 nm and 600 nm at 458 nm excitation. In the co-localization experiments with the addition of different hosts, living HeLa cells were incubated with dyes (0.5 μM), host (1 μM for CB[7], 10 μM for CB[8]) and different commercial organelle makers (lipid droplets markers (Nile Red, 50 nM) or mitochondria marker (Mito-tracker Green, 100 nM)) for 10 min, respectively. The images were captured at the same conditions.

1.6. Computational details

Density functional theory (DFT) at the B3LYP/6-31G(d) level were used to optimize the geometries of dye **NR-Ad**, host CB[7] and the complex **NR-Ad @ CB[7]** at

the ground state using the Gaussian program package.⁴ The electron cloud distribution, energy gap and dipole moment were obtained. All of the calculated structure were at the minimum of local energy. Water was used as the solvents (CPCM model).

2. Tables

Table S1. The electron cloud distribution for the HOMO and LUMO, energy gap and dipole moments of **NR-Ad**, **CB[7]** and **NR-Ad@CB[7]**.

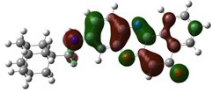
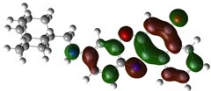
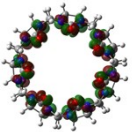

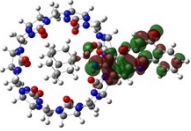
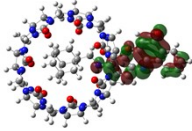
molecule	HOMO	LUMO	ΔE_{H-L} (eV)	Dipole moment (Debye)
NR-Ad	 -3.285 eV	 -0.109 eV	3.176	6.377
CB[7]	 -3.561 eV	 3.486 eV	7.047	0.131
NR-Ad@CB[7]	 -2.456 eV	 0.456 eV	2.912	13.397

Table S2. Optical properties of dye **LDs-NPAd2** in water before and after adding **CB[7]** or **CB[8]**

dye	$\lambda_{Abs, max}$ ^a	$\lambda_{Em, max}$ ^a	Stokes shift ^a	ϵ ^b	Φ ^c	τ_{ave} ^d
LDs-NPAd2	440	535	95	1.09	5.0	1.6
+ CB[7] ^e	445	540	95	0.89	5.5	*
+ CB[8] ^e	440	528	88	1.76	27.6	10.3

^a Reported in nm.

^b Reported in $\times 10^4 \text{ M}^{-1} \text{ cm}^{-1}$.

^c Reported in %. Coumarin-153 ($\Phi = 0.547$ in ethanol, green) was used as the reference compound.

^d Reported in ns.

^e $[\text{CB}[n]]/[\text{LDs-NPAd2}] = 20$ in PBS.

* Reported in *untested*.

3. Figures

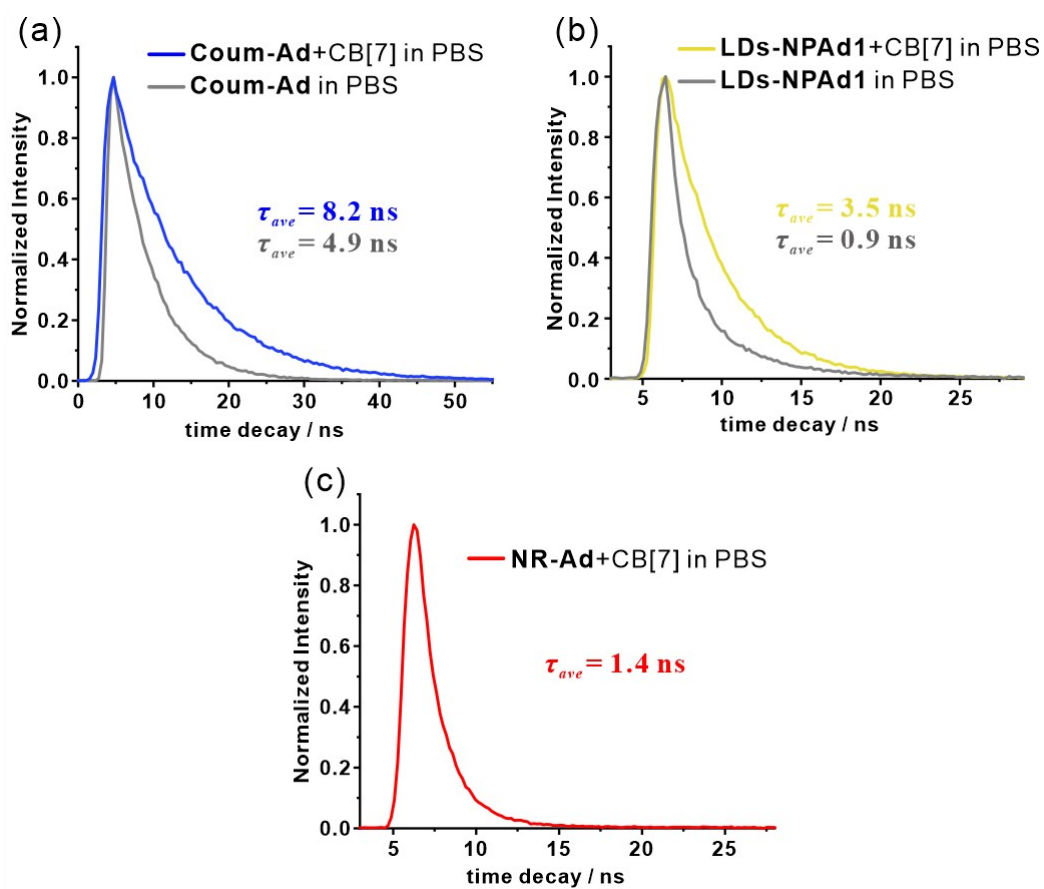


Fig. S1. Fluorescence decay spectra of dyes **Coum-Ad** (a), **LDs-NPAd1** (b), **NR-Ad** (c) before and after the addition of CB[7] in PBS.

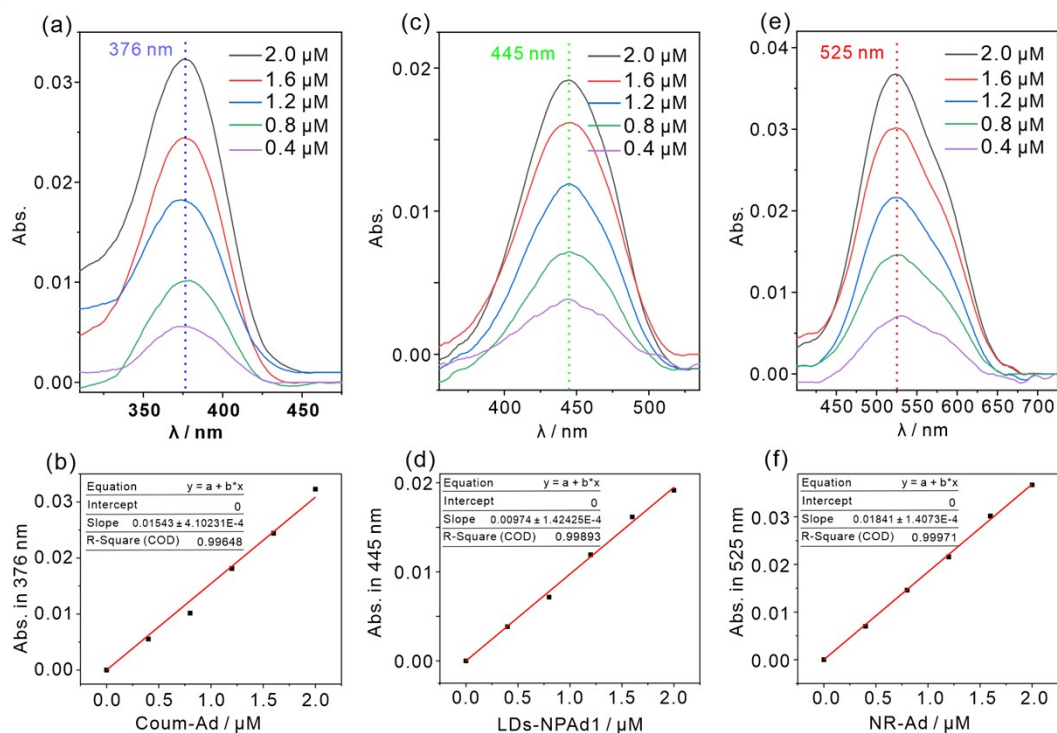


Fig. S2. UV-Vis absorption spectra and standard curves of dyes in different concentrations. (a, b) Coum-Ad; (c, d) LDs-NPAd1; (e, f) NR-Ad.

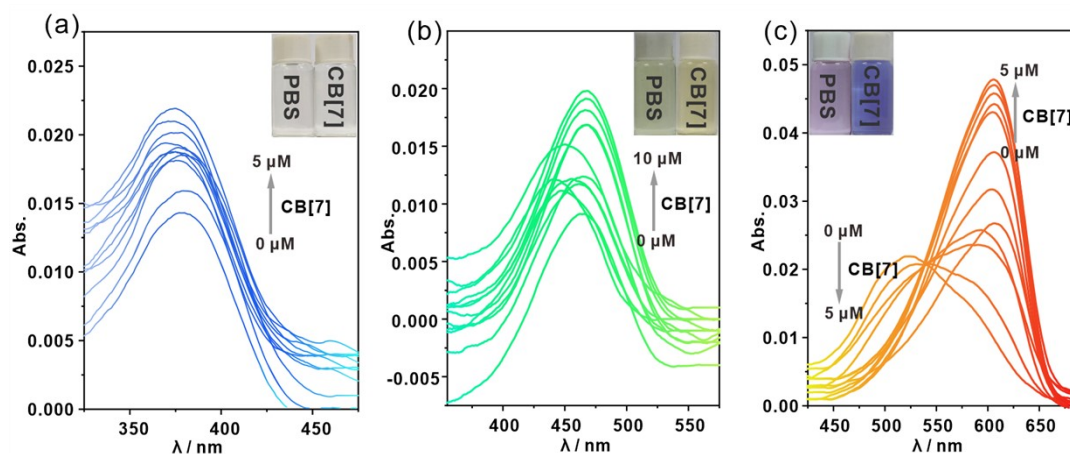


Fig. S3. Absorption spectra of dyes Coum-Ad (a), LDs-NPAd1 (b), NR-Ad (c) with the concentration of 1 μM in different ratios of CB[7] solution. Inset: photographs in sunlight.

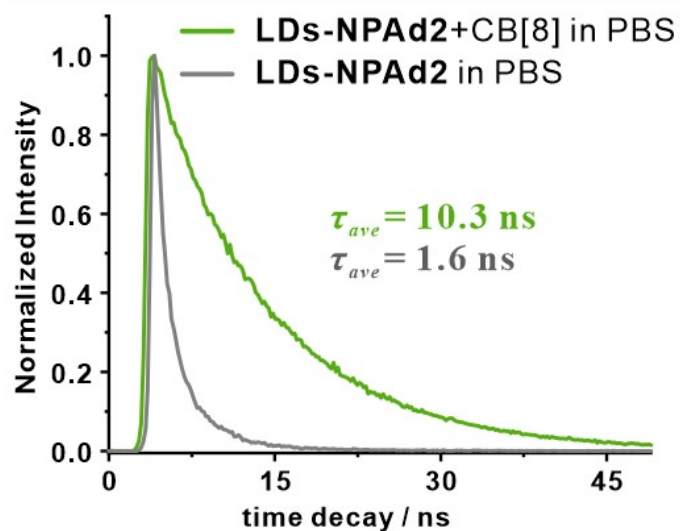


Fig. S4. Fluorescence decay spectrum of dye LDs-NPAd2 before and after the addition of CB[8] in PBS.

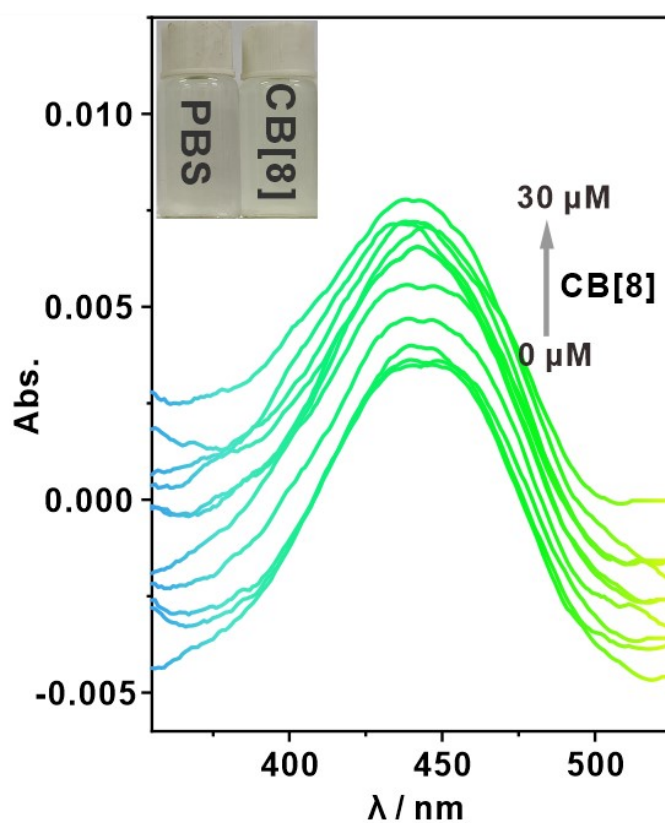


Fig. S5. Absorption spectrum of dye LDs-NPAd2 with the concentration of 1 μ M in different ratios of CB[8] solution. Inset: photograph in sunlight.

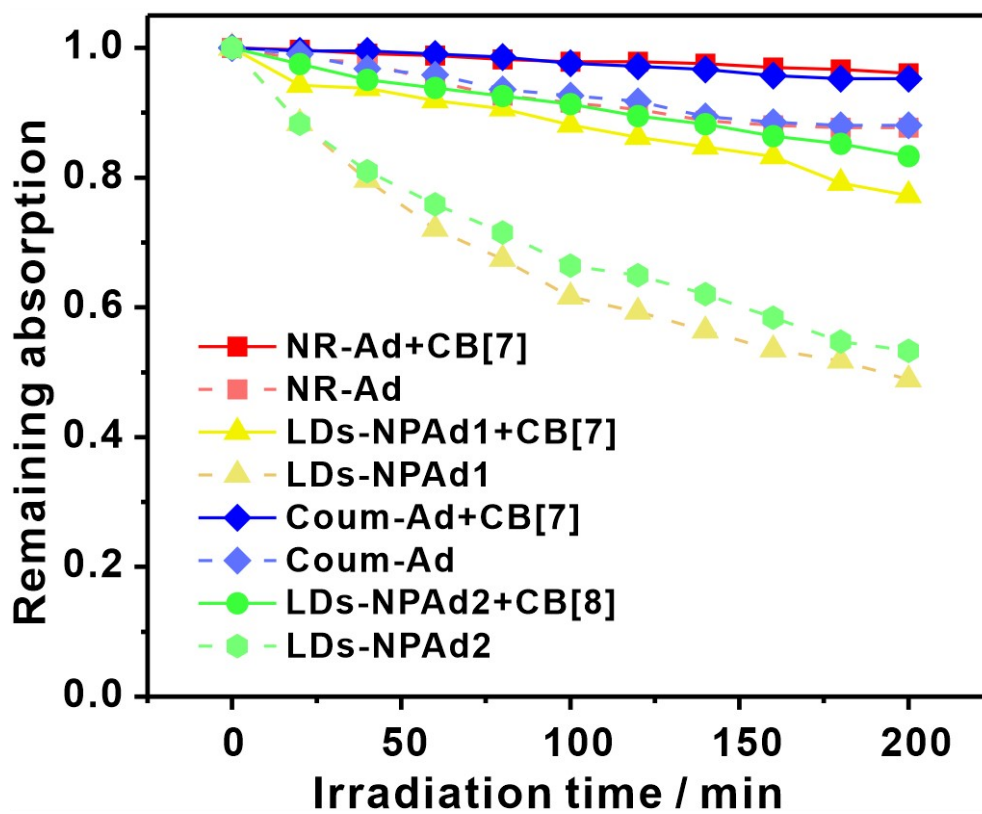


Fig. S6. Photostability of dyes Coum-Ad, LDs-NPAd1, NR-Ad and LDs-NPAd2 with the presence and absence of CB[n] in acetonitrile.

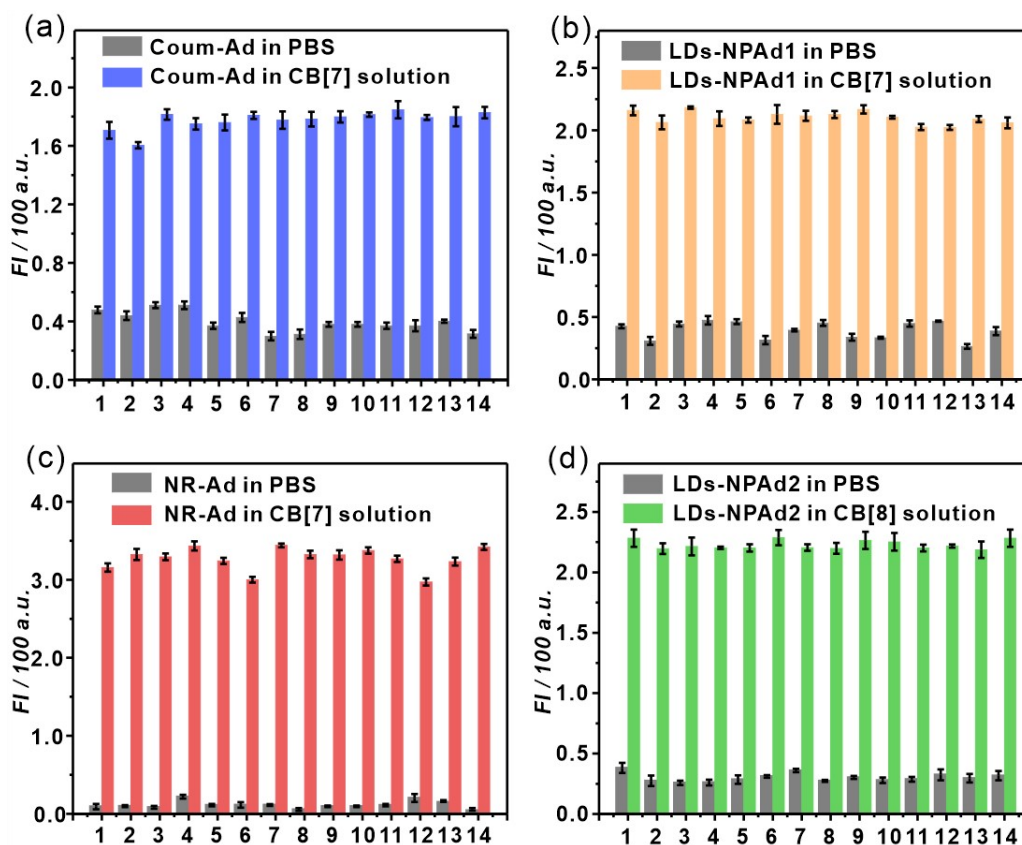


Fig. S7. Selective experiments of dyes **Coum-Ad** (a), **LDs-NPAd1** (b), **NR-Ad** (c), **LDs-NPAd2** (d) with concentration of 1 μM toward different analytes (100 μM) in PBS containing 1% DMSO before and after the addition of CB[7] (2 μM) or CB[8] (20 μM). 1: Blank, 2: Ba²⁺, 3: Cd²⁺, 4: Co²⁺, 5: Cu²⁺, 6: Mn²⁺, 7: Ni²⁺, 8: Pd²⁺, 9: K⁺, 10: CO₃²⁻, 11: SO₄²⁻, 12: Cys, 13: Gly, 14: Lys. **Coum-Ad** was excited at 380 nm, slit widths: 5 nm/3 nm; **LDs-NPAd1** was excited at 466 nm, slit widths: 5 nm/3 nm; **NR-Ad** was excited at 605 nm, slit widths: 5 nm/3 nm; **LDs-NPAd2** was excited at 440 nm, slit widths: 5 nm/3 nm. The data were shown as mean \pm SD (n = 3).

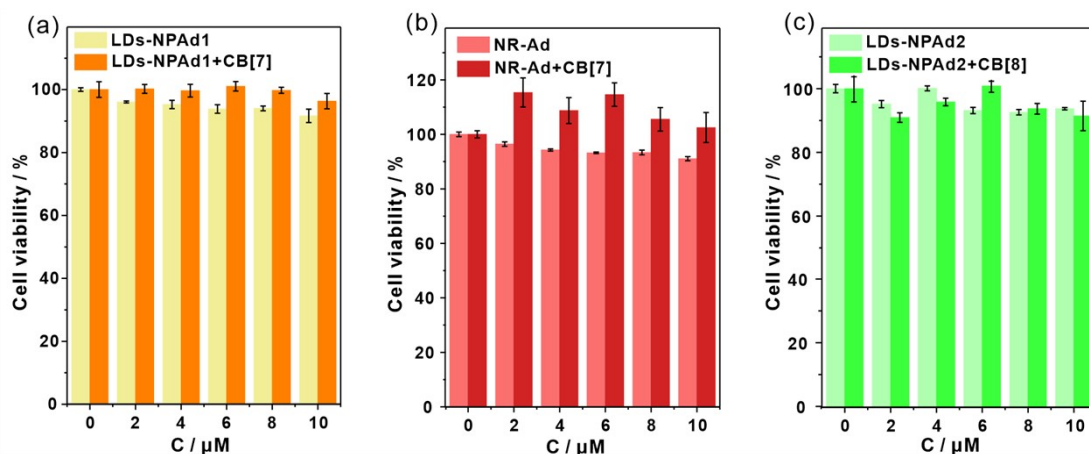


Fig. S8. Cell viabilities of living HeLa cells incubated with dyes in different concentration gradients (0, 2, 4, 6, 8 and 10 μM) before and after the addition of CB[7] (2 eq) or CB[8] (20 eq). The data were shown as mean \pm SD ($n = 3$).

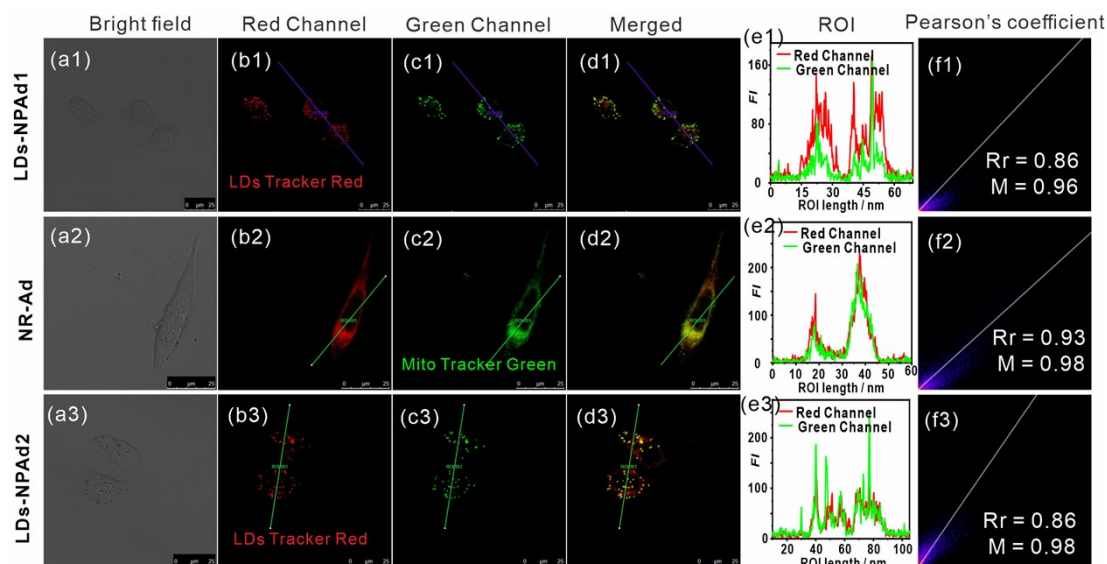


Fig. S9. Colocalization images of living HeLa cells with dyes (0.5 μM), CB[7] (1.0 μM) or CB[8] (10 μM) and corresponding commercial organelle-makers. (a1-a3) The brightfield images of living HeLa cells; (b1-b3) confocal images in red channel; (c1-c3) confocal images in green channel; (d1-d3) The merged images of (b1-b3) and (c1-c3); (e1-e3) The fluorescent intensity for the linear regions of interest (ROIs); (f1-f3) The fluorescent intensity correlation plots.

4. References

1. H. J. Liu, G. Zhang, Y. J. Xu, R. Sun and J. F. Ge, *Chem. Eur. J.*, 2023, **29**, e202302782.
2. K. Rurack and M. Spieles, *Anal. Chem.*, 2011, **83**, 1232-1242.
3. K. Nawara and J. Waluk, *Anal. Chem.*, 2017, **89**, 8650-8655.
4. M. J. Frisch, G. W. Trucks, H. B. Schlegel, G. E. Scuseria, M. A. Robb, J. R. Cheeseman, G. Scalmani, V. Barone, B. Mennucci, G. A. Petersson, H. Nakatsuji, M. Caricato, X. Li, H. P. Hratchian, A. F. Izmaylov, J. Bloino, G. Zheng, J. L. Sonnenberg, M. Hada, M. Ehara, K. Toyota, R. Fukuda, J. Hasegawa, M. Ishida, T. Nakajima, Y. Honda, O. Kitao, H. Nakai, T. Vreven, J. A. Montgomery, Jr., J. E. Peralta, F. Ogliaro, M. Bearpark, J. J. Heyd, E. Brothers, K. N. Kudin, V. N. Staroverov, T. Keith, R. Kobayashi, J. Normand, K. Raghavachari, A. Rendell, J. C. Burant, S. S. Iyengar, J. Tomasi, M. Cossi, N. Rega, J. M. Millam, M. Klene, J. E. Knox, J. B. Cross, V. Bakken, C. Adamo, J. Jaramillo, R. Gomperts, R. E. Stratmann, O. Yazyev, A. J. Austin, R. Cammi, C. Pomelli, J. W. Ochterski, R. L. Martin, K. Morokuma, V. G. Zakrzewski, G. A. Voth, P. Salvador, J. J. Dannenberg, S. Dapprich, A. D. Daniels, O. Farkas, J. B. Foresman, J. V. Ortiz, J. Cioslowski, and D. J. Fox, *Gaussian 09, Revision C.01*, Gaussian, Inc., Wallingford CT, 2010.